USGS
science for a changing world

Isostatic Gravity Map with Geology of the Santa Ana 30’ x 60’ Quadrangle, Southern California

By V.E. Langenheim, Tien-Chang Lee, Shawn Biehler, R.C. Jachens, and D.M. Morton

2006

Scientific Investigations Map 2951

U.S. Department of the Interior
U.S. Geological Survey

Abstract

This report presents an updated isostatic gravity map, with an accompanying discussion of the geologic significance of gravity anomalies in the Santa Ana 30 by 60 minute quadrangle, southern California. Comparison and analysis of the gravity field with mapped geology indicates the configuration of structures bounding the Los Angeles Basin, geometry of basins developed within the Elsinore and San Jacinto Fault zones, and a probable Pliocene drainage network carved into the bedrock of the Perris block. Total cumulative horizontal displacement on the Elsinore Fault derived from analysis of the length of strike-slip basins within the fault zone is about 5-12 km and is consistent with previously published estimates derived from other sources of information. This report also presents a map of density variations within pre-Cenozoic metamorphic and igneous basement rocks. Analysis of basement gravity patterns across the Elsinore Fault zone suggests 6-10 km of right-lateral displacement. A high-amplitude basement gravity high is present over the San Joaquin Hills and is most likely caused by Peninsular Ranges gabbro and/or Tertiary mafic intrusion. A major basement gravity gradient coincides with the San Jacinto Fault zone and marked magnetic, seismic-velocity, and isotopic gradients that reflect a discontinuity within the Peninsular Ranges batholith in the northeast corner of the quadrangle.

Introduction

An important objective of geologic mapping is to provide information not only about geology exposed at the surface but also about geology below the Earth's surface by projecting rock types, stratigraphy, and structures into the subsurface. Geophysical data and analysis are useful tools for achieving this objective. This isostatic gravity map provides a three-dimensional perspective to the geologic mapping of the Santa Ana 30 by 60 minute quadrangle. The isostatic gravity map reflects density variations of rock units in the upper and middle crust. Interpretation of these anomalies provides information on the depth of Cenozoic basins and on the nature of pre-Cenozoic basement rocks. The isostatic gravity map overlain on geology, in concert with information from wells and other geophysical data, provides constraints on the subsurface geology, particularly on the geometry of basins developed along strike-slip faults and the three-dimensional delineation of basement rock types and structure. These data can also be used to

constrain both strike-slip and dip-slip offsets of the major strike-slip faults in the quadrangle.

This map represents more than an update of the isostatic gravity map by Langenheim and others (1991) in that our earlier map only showed gravity contours on a topographic base and did not provide any analysis of the gravity field with respect to the surficial geology. Here we not only provide an updated version of the gravity field, but we also describe the significance of various features expressed in the isostatic gravity field. The geologic significance of the gravity anomalies is enhanced by filtering and analysis of the gravity field.

Geologic Setting

The Santa Ana quadrangle is located in the northwestern part of the Peninsular Ranges province. Peninsular Ranges batholithic rocks underlie most of the quadrangle, except for the extreme northeast corner, which is underlain by basement rocks of the Transverse Ranges province. Morton (2004) divided the quadrangle into three main blocks by the active Elsinore and San Jacinto strike-slip faults (fig. 1); from west to east are the Santa Ana Mountains, Perris, and San Jacinto Mountains blocks. Much of the discussion herein is from Morton (2004), where more details on the geologic setting and rock types can be found.

The Santa Ana Mountains block contains from west to east the southern part of the Los Angeles Basin, which consists of a thick sequence of Neogene sedimentary rocks (Yerkes and others, 1965), and the complexly faulted anticlinal structure of the Santa Ana Mountains, which has a core of Mesozoic metasedimentary rocks and Cretaceous Peninsular Ranges batholithic rocks.

The Perris block is a rectangular area of low relief located between the Elsinore and San Jacinto Faults. It is underlain by prebatholithic metasedimentary rocks intruded by the Peninsular Ranges batholithic rocks. A generally thin section of nonmarine, mainly Quaternary sediments locally mantle the basement rocks, while Cretaceous and Paleogene sedimentary strata lap across the western edge of the block (McCulloh and others, 2000) and thus may be present in basins along the Elsinore Fault. This block remained relatively undeformed during the Neogene.

The San Jacinto Mountains block is located northeast of the San Jacinto fault. Miocene to Quaternary sedimentary rocks form a thick sequence overlying plutons of the Peninsular Ranges batholith and older metamorphic rocks. Outcrops of basement are limited to small exposures in the southeast part of the block within the Santa Ana quadrangle. The San Jacinto Mountains block is bounded to the northeast by the Banning fault, which forms the southwest boundary of Transverse Ranges province basement in the extreme northeast corner of the quadrangle.

Gravity Data

The isostatic gravity map was created from 8,805 gravity stations. Since publication of Langenheim and others (1991) gravity map, these data include 256 new gravity stations collected by the U.S. Geological Survey; 4,943 stations collected by University of California, Riverside; and 229 National Geodetic Survey stations—the remaining data are derived from Langenheim and others (1991). Gravity stations are non-uniformly distributed in the region. There is very dense station spacing (>10 stations per km^2)in the Perris block resulting from detailed studies presented in various master's theses of the University of California, Riverside (Perina, 1993; Miller, 1996; Zawila, 1996; Aiken, 1998) and sparse coverage in the more mountainous and remote areas (< 0.5 stations per km^2).

The datum of observed gravity for this map is the International Gravity Standardization Net of 1971 (IGSN 71) that was described by Morelli (1974); the reference ellipsoid is the Geodetic Reference System of 1967 (GRS67; International Association of Geodesy and Geophysics, 1971). The observed gravity data were reduced to free-air anomalies using standard formulas (for example, Telford and others, 1976). Bouguer, curvature, and terrain corrections to a radial distance of 166.7 km were applied to the free-air anomaly at each station to determine the complete Bouguer anomalies at a standard reduction density of 2,670 kg/m^3 (Plouff, 1977). An isostatic correction was then applied to remove the long-wavelength effect of deep crustal and/or upper mantle masses that isostatically support regional topography. The isostatic correction assumes an Airy-Heiskanen model of isostatic compensation (Heiskanen and Vening-Meinesz, 1958). An isostatic correction using a sea-level crustal thickness of 25 km, a crustal density of 2,670 kg/m^3, and a mantle-crust density contrast of 400 kg/m^3 was applied to the gravity data to

remove long-wavelength crustal gravity effects of topographic loading (Jachens and Griscom, 1985). The resulting isostatic residual gravity values should reflect lateral variations of density within the mid- to upper crust (Simpson and others, 1986); this statement is supported by the favorable comparison of the observed isostatic gravity field with that predicted from seismic velocities in southern California (Langenheim and Hauksson, 2001). A color-contour representation of the isostatic gravity field is shown in figure 2.

Accuracy of the data is estimated to be about ±0.1 to ±0.5 mGal based on comparison of observed gravity values at duplicate stations from different data sources and expected error resulting from the total terrain correction. Total terrain corrections for the stations collected for this study ranged from 0.3 to 39.8 mGal, with an average of 1.3 mGal. If the error from the terrain correction is considered to be 5 to 10 percent of the terrain correction, the largest error expected for the data is 4.0 mGal. However, the possible error caused by the terrain correction is small (less than 0.2 mGal) for most of the stations.

The addition of new data since publication of the map of Langenheim and others (1991) increases the resolution of gravity anomalies, particularly in the eastern part of the quadrangle (fig. 3). Differences in the gravity field are as high as 5-6 mGal in the eastern part of the map, although the major gravity anomalies were present in the older version of the map. The addition of new data tightens gravity gradients and produces higher frequency anomalies; these results allow for more meaningful interpretations when filtered versions of the gravity field are analyzed.

To help emphasize gravity anomalies caused by shallow crustal sources (< 2-3 km), we subtracted a numerically derived regional field from the actual data. The regional field was computed by analytically continuing the observed gravity data to a surface 1 km higher than that on which the measurements were made, an operation that tends to smooth the data by attenuating short-wavelength anomalies (Blakely, 1995). The resulting residual gravity field is shown in figure 4.

Another method (Jachens and Moring, 1990) was used to separate that part of the gravity field caused by Cenozoic deposits from that caused by variations in the density of the basement rocks (defined here as pre-Cenozoic igneous and metamorphic rocks). The

method was modified to include constraints based on well information and depths to basement derived from other geophysical data (B.A. Chuchel, written commun., 1995). The inversion method assumes no lateral density variations within the basin fill. A density-depth function based on the Los Angeles Basin was used for the map area, except for basin fill northeast of the Perris block, where a modified density-depth function based on the San Bernardino Valley was used (table 1).

Table 1. Density-depth function for calculating basin depths

	Los Angeles Basin*		Northeast of Perris Block**
Depth Range (m)	Density contrast (kg/m^3)	Depth Range (m)	Density contrast (kg/m^3)
0-500	-600	0-100	-550
500-1000	-550	100-200	-430
1000-1500	-480	200-600	-360
1500-2500	-390	600-1500	-300
>2500	-250	>1500	-230

* Density-depth function from calculation of densities from average porosity curve of Los Angeles and Ventura basins (McCulloh, 1967, *his* Fig. 4)
**Modified from that used in Anderson and others (2004) in San Bernardino Valley

Two products result from this inversion: (1) thickness of Cenozoic deposits (fig. 5) and (2) the basement gravity field (fig. 6). The basement gravity field is reasonably well constrained by measurements made on basement, except for the western part of the quadrangle in the Los Angeles Basin where the inversion is constrained by just a few scattered drillholes that penetrated basement. Comparison of predicted depths from the inversion model with depths to basement encountered in wells indicates a mean difference of 2 m, with a standard deviation of 34 m. The worst misfit (up to 237 m or 17 percent of the basement depth) occurred within the steep gravity gradient coincident with the Whittier Fault.

Description of Gravity Anomalies

Many of the gravity anomalies of the Santa Ana quadrangle can be explained by density contrasts expressed in the surface geology (see map). The most significant density contrast is that between dense crystalline basement rocks and lower density Cenozoic sedimentary rocks and deposits. Outcrops of basement rocks are generally associated with gravity highs, in contrast to the large gravity lows present over thick sedimentary fill

in the Los Angeles Basin and San Jacinto Valley. The isostatic gravity values range from a low of -49 mGal over the Los Angeles Basin along the western margin of the map to a high of +21 mGal near Bachelor Mountain in the southeast part of the map (see map; fig. 2). The gravity data provide information on major structural features such as the Newport-Inglewood, Elsinore, San Jacinto, and Whittier Faults (fig. 1). These structural features bound the main basins in the quadrangle.

Basins

Los Angeles Basin

The eastern part of the Los Angeles Basin central synclinal trough coincides with the lowest gravity values on the quadrangle (see map; fig. 2). Structures that form the northern and eastern margins of the basin are well expressed by gravity anomalies. The northern margin of the present-day structural basin as defined by Yerkes (1972) is the Whittier Fault, a north-dipping, reverse, right-oblique fault (Ziony and Yerkes, 1985). Gravity data are consistent with north-side-up displacement on the Whittier Fault; there is nearly 20 mGal of relief across the fault between longitude 117° 54'W. and 117° 48'W., that coincides with the maximum vertical separation (about 4.3 km) of upper Miocene rocks across the fault (Yerkes, 1972). The highest gravity values north of the fault (figs. 2, 4) coincide with shallow basement rocks (1,040-1,500 m) penetrated by oil wells in the hanging wall of the fault (Yerkes, 1972; Wright, 1991) and apparently outline the area of maximum vertical separation on the fault. The location of the fault within the middle of the gravity gradient suggests a steep (>45°) dip. Eastward from the area of highest gravity values, the amplitude of the gravity gradient decreases to zero at about longitude 117° 45'W. Further east, in the Santa Ana Canyon area, the sense of dip-slip displacement, the dip of the Whittier Fault, and the direction of the gravity gradient are reversed as the Whittier Fault forms the northern margin of the Santa Ana Mountains (Wright, 1991; McCulloh and others, 2000). The position of the Whittier Fault at the base of the gravity gradient indicates a southwest dip of the fault. At the northeast margin of the Santa Ana Mountains, the Whittier Fault merges with the Elsinore Fault (see map; fig. 2). The position of the Whittier and Elsinore Faults at the base of the northeast-facing gravity gradient is consistent with reverse to thrust component of slip on these faults that may be a mechanism for generating topographic relief of the northern

Santa Ana Mountains. Compression and uplift are expected in this region where the strike of the Whittier and northernmost Elsinore Faults are more westerly relative to the average northwest strike of these dominantly right-lateral, strike-slip systems.

The southeastern margin of the Los Angeles Basin is marked by gravity highs over the southeastern Santa Ana Mountains and the San Joaquin Hills (fig. 2). The gravity high over the Santa Ana Mountains is expected because of its anticlinal structure and the Mesozoic basement rocks exposed in its core. However, the large amplitude of the gravity high over the San Joaquin Hills and Santa Ana Shelf is surprising because basement in this area is buried by as much as 3 km of Paleogene and younger sedimentary rocks (Schoelhamer and others, 1981). Gravity values in the San Joaquin Hills and Santa Ana Shelf are as much as 10-15 mGal higher than values measured on basement in the northern part of the Perris block and are among the highest measured in the quadrangle (figs. 2, 6). The source of these high gravity values must reside in the basement (McCulloh, 1960) and will be discussed later. Superposed on the pronounced San Joaquin gravity high are local north- to northwest-striking anomalies (figs. 2, 4). A local gravity low between the Shady Canyon and Pelican Hills Faults (**L1** on fig. 4) reflects a 2-km-deep trough of Neogene strata formed by block faulting (Wright, 1991). Southwest of the Neogene trough is a narrow gravity high nestled between the Pelican Hills and the Newport-Inglewood Faults that reflects shallow basement (fig. 5).

East of the San Joaquin Hills gravity high is the gravity low of the Capistrano embayment (**CE** on fig. 4), which contains more than 2 km of Cretaceous and younger sedimentary rocks (Wright, 1991, his figure 4). The Cristianitos Fault, a poorly understood Neogene normal fault that forms the eastern margin of the syncline, coincides with a north-striking gravity gradient that is highlighted in the residual gravity map (fig. 4). This map also highlights a north- to north-northwest-striking structural grain within the San Joaquin Hills that extends as far west as longitude 117° 45' W. This north-striking grain appears truncated by a northwest-striking grain that is parallel to the strike of the northern boundary of the San Joaquin Hills gravity high. The gravity field maps a trough of thick basin fill nestled between the exposed basement rocks of the Santa Ana Mountains and the northern margin of the San Joaquin gravity high (**L2** on figs. 4, 5).

The residual gravity map also highlights a gravity high that reflects intrabasinal structure within the Los Angeles Basin. The Anaheim Nose, an entirely concealed, west-northwest-plunging ridge, is an old Miocene structural element within the basin that shows evidence for repeated movements (McCulloh and others, 2000). It is expressed as a gravity high that extends from the San Joaquin gravity high toward the west-northwest across the quadrangle (figs. 2, 4). It is best expressed on the residual gravity map (fig. 4); its expression on the basin thickness map is complicated by uncertainties in the basement gravity field. Although the southwestern edge of the Anaheim Nose has been projected to be the extension of the Shady Canyon Fault (Wright, 1991; McCulloh and others, 2000), the residual gravity indicates that the two structures differ in strike by as much as 30°.

Chino-Elsinore Trough

The Chino-Elsinore trough is an elongate, topographically low region bounded on the southwest by the Elsinore and Chino Fault zones (fig. 1; Woodford and others, 1944; Gray, 1961). The physiographic low is mirrored by relatively low gravity values. Low gravity values extend west across the Chino Fault into the eastern Puente Hills as far west as longitude 117° 45'W. The western margin of the gravity low may outline the westernmost extent of Paleogene and thick Neogene strata in the subsurface and coincides approximately with the eastern edge of an area where Paleogene strata have been stripped away (McCulloh and others, 2000). The eastern margin of the gravity low is marked by the "Chino Hingeline" Fault (Wright, 1991), also known as the "Central Avenue Fault" (Woodford and others, 1944; McCulloh and others, 2000), which has no apparent surface expression. This structure has more than 1,000 m of post-Paleogene structural relief (McCulloh and others, 2000) and is well delineated by a linear gravity gradient (fig. 2). This feature is particularly evident in the residual gravity gradient (fig. 4). Based on the correlation of the fault and its residual gravity expression, we extend the fault 10 km southeast of its trace that was mapped by drillhole data (Woodford and others, 1944; McCulloh and others, 2000) where it merges with the Elsinore Fault (fig. 4). Furthermore, the fault can be extended 5-6 km to the northwest of its mapped trace where the gravity gradient may step to the right near the northern edge of the quadrangle. The "Chino Hingeline" (or "Central Avenue") Fault thus appears to be an extension of

the N. 40° W. strike of the southeast part of the Elsinore Fault, perhaps sharing an early Neogene zone of weakness along which the present Elsinore Fault developed (Wright, 1991, p. 46).

The Chino Fault bounds the eastern margin of the Puente Hills (fig. 1) and it is a southwest-dipping, oblique reverse fault along its southern half (Durham and Yerkes, 1964; McCulloh and others, 2000). Well data indicate that the fault dips about 60° southwest and has as much as 0.7 km of stratigraphic separation (Durham and Yerkes, 1964). This geometry should produce a 12 mGal anomaly along a northeast-facing gravity gradient using the infinite-slab calculation that assumes a density contrast of 400 kg/m^3. However, the Chino Fault is located at the base of a southwest-facing gravity gradient, except where it is inferred at its southeastern end near its intersection with the Whittier and Elsinore Faults. This discrepancy is resolved if the hanging wall of the fault consists of a narrow (< 2 km) anticline that is accompanied by a wide syncline in the hanging wall, as suggested by cross-sections across the fault (Durham and Yerkes, 1964). The lack of gravity expression across the fault suggests that the uplifted basement rocks along the Chino Fault may be less than 1-2 km wide and would not be resolved given the present distribution of gravity stations across the fault. Alternatively, the lack of gravity expression may suggest that the Chino Fault formed originally as a basin margin fault that has been reactivated as a reverse fault or that an earlier history led to erosion of Tertiary sedimentary rocks on the east side of the fault.

Basins along the Elsinore and San Jacinto fault zones

Both of the major Neogene strike-slip faults that cut across the Santa Ana quadrangle have local, well-developed basins or grabens along their traces. Southeast of the Chino-Elsinore trough are two well-defined strike-slip basins along the Elsinore Fault zone. The northwestern pull-apart basin (**EB** on fig. 4) is centered on Lake Elsinore and is bounded on the northeast by the Glen Ivy North Fault and on the southwest by the Elsinore Fault. The southeastern basin (**MB** on fig. 4) is centered near the town of Murrieta and is bounded by the Wildomar and Willard Faults on its northeast and southwest margins, respectively. The basin thickness map (fig. 5) indicates that both basins are about 2-3 km wide, 8-12 km long, and 1-2 km deep, consistent with results of earlier studies (Hull, 1990; Moyle and Downing, 1983; Rodeick and Nelson, 1980,

written commun.). Basin fill is late Pliocene and younger in age (Kennedy, 1977). The gravity gradients (figs. 2, 4) indicate that the bounding faults are near-vertical to steeply dipping (Hull and Nicholson, 1992). The basin lengths of 10-12 km are compatible with a total strike-slip offset of 10-12 km, although a strike-slip basin of this length could be generated by smaller offset if the present basin resulted from the merging of shorter, en echelon basins (Aydin and Nur, 1982). However, the relatively linear boundaries of the basins and the length to width ratio of about 3-to-1 suggest that these are not composite basins. Furthermore, the estimates of horizontal separation from the basin lengths are compatible with other estimates from offsets of Paleogene depositional patterns (8-9 km; McCulloh and others, 2000) and of basement contacts, Miocene basalt, and K-Ar ages (10-15 km as summarized in Hull and Nicholson, 1992). Another small gravity low (**B1** on fig. 4) about 15 km northwest of Lake Elsinore may reflect another strike-slip basin within the Elsinore Fault zone. Its length is only about 5 km, or about half that of the Lake Elsinore and Murrieta Basins; this shorter length is perhaps due to compression that resulted from a more westerly strike in the Elsinore Fault zone or from a younger age of initiation.

Applying this hypothesis to the Chino Fault, which appears to be an extension of the Elsinore Fault, we speculate that the linear gravity lows within the Chino-Elsinore trough also formed as a result of right steps in the Elsinore-Chino Fault zones. Thus, maximum offset is approximately 10-12 km, comparable to the amount of total offset on the Elsinore Fault, but substantially more than that inferred for the Chino Fault (<2.5 km; McCulloh and others, 2000).

In the southeast corner of the quadrangle, the Temecula Basin (fig. 1) extends east from the Elsinore fault zone. The northern margin of the basin is the Hot Springs (Murrieta) Fault. An east-oriented gravity low (fig. 2) reflects the low-density sedimentary fill of the basin. Two small gravity highs in the basin (see map; **H1** and **H2** on fig. 4) reflect either the presence of gabbro beneath the basin fill or undulations on the basement surface.

Another prominent strike-slip basin is located between the strands of the San Jacinto Fault zone in the San Jacinto Valley (fig. 1). The gravity low associated with the strike-slip basin in the valley extends beyond the eastern edge of the Santa Ana quadrangle; the

lowest values are 5 km east of the quadrangle's eastern edge. Inversion of gravity data indicates that there are two, 10-km-long sub-basins beneath the San Jacinto Valley (Langenheim and others, 2002); only the northwestern sub-basin is present in the Santa Ana quadrangle. The sub-basin is bounded by the Casa Loma and Claremont Faults on its southwest and northeast margins, respectively, and is as much as 4 km deep (fig. 5). Seismic-reflection data at the north end of the graben identified an intrabasinal fault, the presence of which suggests that the basin beneath San Jacinto Valley is comprised of coalescing sub-basins (Park and others, 1995).

Northeast of the gravity low associated with the San Jacinto strike-slip basin is a northwest-striking gravity high located over the San Timoteo Badlands (fig. 4). The highest gravity values are at the southeast end of the gravity high where basement rocks are exposed. The amplitude of the gravity high diminishes progressively to the northwest where it disappears about 5 km from the northern edge of the quadrangle. This anomaly reflects a northwest-plunging, basement-cored anticline. Kendrick and others (2002) attributed formation of the anticline to a restraining bend in the San Jacinto Fault. The location of maximum uplift based on their geomorphic analysis approximately coincides with the northwest end of the San Timoteo Badlands gravity high.

Northeast of the San Timoteo Badlands, gravity values decrease into a northwest-striking gravity low, which contains nearly the lowest values of the quadrangle. This gravity low reflects the Beaumont Basin (fig. 2), which is about 2-3 km deep (fig. 5). Allen (1957) suggested the presence of a deep basin beneath this area based on one oil well. The genesis of this basin is unknown, but it could be the offset equivalent of the Coachella Valley Basin, displaced approximately 25 km right-laterally by the Banning Fault (Langenheim and others, 2005). Other possible origins for this basin include formation as a strike-slip basin or as a synformal depression.

Channels in the Perris block

Closely spaced gravity stations in the eastern Perris block delineate linear, narrow channel-like depressions that appear to form part of a Pliocene (and possibly as old as middle Cenozoic; Woodford and Gander, 1977) drainage network. These channels are subtle features on the isostatic gravity map (fig. 2), but they are well expressed on the residual gravity and the basin thickness maps (figs. 3, 5). The channels are as much as

300-400 m deep (fig. 5), are graded to the southwest, and converge toward Sun City. The channels were probably eroded into the basement before formation of the San Jacinto graben because they appear to be beheaded by the Casa Loma Fault and because of probable offset equivalent channels on the northeast side of the San Jacinto Fault zone (J. Matti, oral commun., 2005). Another possible paleochannel (**c?** on fig. 4) strikes west-southwest across the Perris block 8 km southeast of the present channel of the Santa Ana River, although more detailed data are needed to confirm this speculation.

Pre-Cenozoic Basement

The inversion method produces not only a basin thickness map but also a map of the basement gravity field (fig. 6). The basement gravity field reflects the density of pre-Cenozoic rocks exposed or buried beneath basins within the quadrangle. Caution should be used in interpreting basement gravity anomalies over basins without well control or independent control from other geophysical data. For this reason, the following discussion is limited to areas where pre-Cenozoic rocks are exposed or where several wells or geophysically determined depths to basement exist.

San Joaquin Hills-Anaheim Shelf

The gravity high in the San Joaquin Hills (fig. 6) cannot be explained by density contrasts in the surficial geology or by variations in thickness of the Cenozoic deposits and therefore must be caused by density variations in the basement. This body is well expressed in the basement gravity (fig. 6), although the amplitude and areal extent of its anomaly may be exaggerated because the assumed density contrasts within the overlying basin fill may be overestimated. The density-depth relationship used for the basin inversion assumes that the top layer consists of Quaternary deposits. In the San Joaquin Hills, many of the surficial deposits are Miocene and older (units Ts, Tt, Tv on map) and most likely denser because of compaction. The gravity high also coincides with a prominent magnetic high (Jachens and Dixon, 1991), which continues (although more subdued) to the northwest. McCulloh (1960) attributed the source of this gravity high to a deep-seated, high-density source, such as gabbro. The geologic affinity of this dense, magnetic rock is not known from direct evidence. Dense mafic rock types include Peninsular Ranges gabbro (McCulloh, 1960; Langenheim and Jachens, 1993), Mesozoic ophiolite, and igneous intrusives that were the source of Miocene volcanic rocks (Wright,

1991). Based on modeling of magnetic data we identify the source of this gravity high located over the San Joaquin Hills as gabbro of the Peninsular Ranges batholith (Langenheim and Jachens, 1993). This model indicates that the source extends to at least 10 km depth, with a northeast edge dipping about 45° to the northeast. This geometry is similar to that of a major discontinuity within the Peninsular Ranges batholith (fig. 1; Langenheim and others, 2004). The top of the San Joaquin Hills body may be as shallow as 4 km, and the magnetic and gravity anomalies may be the result of two bodies—one very deep body (Peninsular Ranges gabbro) that accounts for the regional magnetic and gravity anomaly and a more shallow body, possibly a source of Tertiary diabase that accounts for the more local magnetic and gravity highs.

Another basement gravity high may be associated with two high-velocity anomalies at 9-18 km depth beneath the Whittier and El Modeno areas attributed to dioritic plutons (Bjorklund and others, 2002). Bjorklund and others (2002) suggest that these plutons are the source of the Glendora Volcanics and diabase sills in the Puente Hills and of the El Modeno Volcanics to the southeast. The basement gravity field, although poorly constrained, does indicate positive values in these areas (> 16 mGal; fig. 6), although these plutons do not apparently produce coincident magnetic anomalies (Jachens and Dixon, 1991), which might be expected for diorites.

Santa Ana Mountains and Perris Block

The Santa Ana Mountains are characterized by low basement gravity and isostatic gravity values (< 0 mGal) that increase in magnitude to the southeast (see map; figs. 2, 6). Not surprisingly, the lowest values coincide with extensive exposures of the Triassic-Cretaceous Bedford Canyon Formation (unit Jbc on map), a slightly metamorphosed sedimentary package, and the Cretaceous Santiago Peak Volcanics (unit Kvsp on map), a heterogeneous assemblage of relatively siliceous volcanic rocks. The lowest values (< -16 mGal) adjacent to the Elsinore Fault may also be affected by the southwest dip of the fault, which would place low-density Tertiary sedimentary rocks beneath basement exposures. In this case, low-density sedimentary rocks beneath crystalline basement represents a condition that is not taken into account by the inversion procedure so the gravity low could be produced by concealed sedimentary rocks rather than reflecting an intrinsic property of the basement itself.

Basement gravity values step to higher values (> 0 mGal) west of Lake Elsinore, roughly coincident with a poorly-exposed northeast-striking geologic structure ("west step" on fig. 6). Southeast of this step the predominant rock types are plutons of the Peninsular Ranges batholith, including gabbro (Kgb), instead of the lower-density, low-grade metasedimentary and hydrothermally altered volcanic rocks that dominate exposures northwest of the step. The higher gravity values also coincide approximately with high-amplitude, coherent magnetic highs (Langenheim and others, 2004) and low initial strontium isotopic ratios of 0.704 or less (Kistler and others, 2003), indicating a more mafic (or primitive) and thus denser rock type.

East of the Elsinore Fault, a similar pattern in the basement gravity is observed in the Perris block (fig. 6). Basement gravity values are lowest in the northwest part of the block, increasing to the southeast. Areas characterized by gravity values less than 0 mGal are underlain by Cretaceous volcanic rocks (for example, Kvem, Kvs on map) and monzogranite (Kmg on map) and are generally devoid of gabbro. Basement gravity and isostatic gravity values exceeding 8 mGal are in the southeast part of the Perris block, where gabbro exposures are abundant (Kgb on map). The area of broad east-oriented gravity highs north of the Temecula Basin reflects the distribution of gabbro extending from the Paloma Valley ring complex (unit Kpv) across French Valley to the area of Skinner Reservoir (see map). The Lakeview Mountains pluton (Klm on map), a compositionally zoned tonalite, is also associated with high basement gravity and magnetic values and low initial strontium ratios (Langenheim and others, 2004). Correlating these patterns of decreasing basement gravity across the Elsinore Fault in the area of Lake Elsinore (west and east steps on fig. 6) suggests about 6-10 km of right-lateral displacement.

San Jacinto Mountains Block

The San Jacinto Mountains block is also characterized by low basement gravity values (<12 mGal). The low basement gravity values are consistently lower than those in the adjacent Perris block. The basement gravity gradient is parallel to the San Jacinto fault zone and is maximized near the Lakeview Mountains (fig. 6). Measured densities in basement rocks across the San Jacinto Fault in this area indicate a contrast of 140 kg/m^3; to match the 30 mGal change across observed the fault, the density contrast must extend

to a depth of 15 km (Langenheim and others, 2004). The basement gravity gradient coincides with magnetic, seismic-velocity, and isotopic gradients that mark a discontinuity within the Peninsular Ranges batholith.

Conclusion

Analysis of gravity data provides constraints on the nature of the subsurface in the Santa Ana 30 by 60 minute quadrangle, California. Important constraints include the basin configuration beneath the various strike-slip basins within the Elsinore and San Jacinto fault zones. The length of the strike-slip basins and correlation of basement gravity patterns across the Elsinore Fault suggests a cumulative horizontal offset of 5-12 km. Gravity data also indicate channel-like depressions in the Perris block that probably formed as part of a Pliocene drainage network. The basement gravity field indicates dense, presumably mafic bodies beneath the San Joaquin Hills and a substantial gradient across the San Jacinto Fault. These gravity variations have important implications not only for the tectonic evolution of the area but also for hydrogeologic studies.

References Cited

Aiken, K.J., 1998, A geophysical investigation of the south Perris block, Riverside County, California: University of California, Riverside, Master's thesis.

Allen, C.R., 1957, San Andreas fault zone in San Gorgonio Pass, southern California: Geological Society of America Bulletin, v. 68, p. 319-350.

Anderson, Megan, Matti, J.C., and Jachens, R.C., 2004, Structural model of the San Bernardino basin, California, from analysis of gravity, aeromagnetic, and seismicity data: Journal of Geophysical Research, v. 109, B04404.

Aydin, A., and Nur, A., 1982, Evolution of pull-apart basins and their scale dependence: Tectonics, v. 1, p. 11-21.

Bjorklund, Tom, Burke, Kevin, Zhou, Hua-Wei, and Yeats, R.S., 2002, Miocene rifting in the Los Angeles basin—evidence from the Puente Hills half-graben, volcanic rocks, and P-wave tomography: Geology v. 30, p. 451-454.

Blakely, R.J., 1995, Potential Theory in Gravity and Magnetic Applications: Cambridge University Press, 441 p.

Durham, D.L., and Yerkes, R.F., 1964, Geology and oil resources of the eastern Puente Hills area, southern California: U.S. Geological Survey Professional Paper 420-B, 62 p.

Fraser, D.M., 1931, Geology of the San Jacinto quadrangle south of San Gorgonio Pass, California: California Mining Bureau Report 27, p. 494-540.

Frick, Childs, 1921, Extinct vertebrate faunas of the badlands of Bautista Creek and San Timoteo Canyon, southern California: University of California Publication, Department of Geological Sciences Bulletin, v. 12, p. 277-409.

Gray, C.H., Jr., 1961, Geology and mineral resources of the Corona South quadrangle: California Division of Mines and Geology Bulletin 178, 120 p.
Heiskanen, W.A., and Vening-Meinesz, F.A., 1958, The Earth and its gravity field: New York, McGraw-Hill Book Company, Inc., 470 p.
Herzig, C.T., 1991, Petrogenetic and tectonic development of the Santiago Peak Volcanics, northern Santa Ana Mountains, California:, Riverside, University of California, Ph.D dissertation , 376 p.
Hull, A.G., 1990, Seismotectonics of the Elsinore-Temecula trough, Elsinore fault zone, southern California: Santa Barbara, University of California, Ph.D. dissertation, 233 p.
Hull, A.G., and Nicholson, Craig, 1992, Seismotectonics of the northern Elsinore fault zone, southern California: Bulletin of the Seismological Society of America, v. 82, p. 800-818.
International Union of Geodesy and Geophysics, 1971, Geodetic Reference System 1967: International Association of Geodesy Special Publication no. 3, 116 p.
Jachens, R.C., and Dixon, E.T., 1991, Aeromagnetic map of the Santa Ana 1:100,000 quadrangle, California: U.S. Geological Survey Open-File Report 91-393, scale 1:100,000.
Jachens, R.C., and Griscom, Andrew, 1985, An isostatic residual gravity map of California—A residual map for interpretation of anomalies from intracrustal sources *in* Hinze, W.J., *ed*., The Utility of Regional Gravity and Magnetic Maps: Society of Exploration Geophysicists, Tulsa, Oklahoma, p. 347-360.
Jachens, R.C., and Moring, B.C., 1990, Maps of the thickness of Cenozoic deposits and the isostatic residual gravity over basement for Nevada: U.S. Geological Survey Open-File Report 90-404, 15 p., 2 plates.
Jennings, C.W., 1994, Fault activity map of California and adjacent areas: California Division of Mines and Geology California Geologic Data Map 6, scale 1:750,000.
Kendrick, K.J., Morton, D.M., Wells, S.G., and Simpson, R.W., 2002, Spatial and temporal deformation along the northern San Jacinto fault, southern California: Implications for slip rates: Bulletin of the Seismological Society of America, v. 92, no. 7, p. 2782-2802.
Kennedy, M.P., 1977, Recency and character of faulting along the Elsinore fault zone in southern Riverside county, California: California Division of Mines and Geology Special Report 131, 12 p.
Kistler, R.W., Wooden, J.L., and Morton, D.M., 2003, Isotopes and ages in the northern Peninsular Ranges batholith, southern California: U.S. Geological Survey Open-File Report 03-489, 181 p.
Langenheim, V.E., Chapman, R.H., Sikora, R.F., Ponce, D.A., and Dixon, E.T., 1991, Isostatic residual gravity map of the Santa Ana 1:100,000-scale quadrangle, California: U.S. Geological Survey Open-File Report 91-555, 1 sheet, scale 1:100,000.
Langenheim, V.E., and Hauksson, Egill, 2001, Comparison of crustal density and velocity variations in southern California: Geophysical Research Letters, v. 28, p. 3087-3090.
Langenheim, V.E., and Jachens, R.C., 1993, Nature of basement rocks under the Los Angeles basin, southern California, as inferred from aeromagnetic data: Geological Society of America Abstracts with Programs, v. 25, p. 66.
Langenheim, V.E., Jachens, R.C., Morton, D.M., and Matti, J.C., 2002, Basins and

plutons along the San Jacinto fault zone, San Bernardino Valley to San Jacinto Valley, southern California: GSA Abstracts with Programs, v. 34, no. 5, p. 86.
Langenheim, V.E., Jachens, R.C., Morton, D.M., Kistler, R.W., and Matti, J.C., 2004, Geophysical and isotopic mapping of preexisting structures that influenced the location and development of the San Jacinto fault zone, southern California: Geological Society of America Bulletin, v. 116, p. 1143-1157.
Langenheim, V.E., Jachens, R.C., Matti, J.C., Hauksson, Egill, Morton, D.M., and Christensen, A.H., 2005, Geophysical evidence for wedging in the San Gorgonio structural knot in the southern San Andreas Fault zone, southern California: Geological Society of America Bulletin, v. 117, no. 11, p. 1554-1572.
McCulloh, T.H., 1960, Gravity variations and the geology of the Los Angeles basin of California: U.S. Geological Survey Professional Paper 400-B, p. B320-B325.
McCulloh, T.H., 1967, Mass properties of sedimentary rocks and gravimetric effects of petroleum and natural-gas reservoirs: U.S. Geological Survey Professional Paper 528-A, 50 p.
McCulloh, T.H.,, Beyer, L.A., and Enrico, R.J., 2000, Paleogene strata of the eastern Los Angeles basin, California: Paleogeography and constraints on Neogene structural evolution: Geological Society of America Bulletin, v. 112, p.1155-1178.
Miller, R.L., 1996, A geophysical study of the Lakeview basin, Riverside County, California: Riverside, University of California, Master's thesis.
Morelli, C. *ed*., 1974, The International Gravity Standardization Net, 1971: International Association of Geodesy Special Publication no. 4, 194 p.
Morton, D. M., 1969, The Lakeview Mountains pluton, southern California batholith: Part I, petrology and structure: Geological Society of America Bulletin, v. 80, p. 1539-1552.
Morton, D.M., 2004, Preliminary digital geologic map of the Santa Ana 30' by 60' quadrangle, southern California: U.S. Geological Survey Open-File Report 99-172, version 2.0. http://pubs.usgs.gov/of/1999/of99-172/
Morton, D.M., and Baird, A.K, 1976, Petrology of the Paloma Valley ring complex, southern California batholith: U.S. Geological Survey Journal of Research, v. 4, n. 1, p 83-89.
Moyle, W.R., Jr., and Downing, D.J., 1983, Bouguer gravity anomaly map of the Temecula area, Riverside county, California in Geology of the northern Elsinore trough: South Coast Geological Society Fieldtrip Guidebook no. 11, p. 164-166.
Osborn, E.F., 1939, Structural petrology of the Val Verde Tonalite, southern California: Geological Society of America Bulletin, v. 50, p. 921-950.
Park, S.K., D. Pendergraft, W.J. Stephenson, K.M. Shedlock, and T.C. Lee, 1995. Delineation of Intrabasin structure in a dilational jog of the San Jacinto fault zone, southern California, Journal of Geophysical Research, v. 100, p. 691-702.
Perina, Tomas, 1993, Geophysical and hydraulic modeling of the Winchester basin, California: Riverside, University of California Master's thesis.
Plouff, Donald, 1977, Preliminary documentation for a FORTRAN program to compute gravity terrain corrections based on topography digitized on a geographic grid: U.S. Geological Survey Open-File Report 77-535, 45 p.
Schoelhamer, J.E., Vedder, J.G., Yerkes, R.F., and Kinney, D.M., 1981, Geology of the northern Santa Ana Mountains, California: U.S. Geological Survey Professional Paper 420-D, 109 p.

Simpson, R.W., Jachens, R.C., Blakely, R.J., and Saltus, R.W., 1986, A new isostatic residual gravity map of the conterminous United States with a discussion on the significance of isostatic residual anomalies: Journal of Geophysical Research, v. 91, p. 8348-72.

Telford, W.M., Geldart, L.O., Sheriff, R.E., and Keyes, D.A., 1976, Applied Geophysics: New York, Cambridge University Press, 960 p.

Woodford, A.O., Shelton, J.S., and Moran, T.G., 1944, Geology and oil possibilities of Puente and San Jose Hills, California: U.S. Geological Survey Oil and Gas Investigations Preliminary Map 23, scale 1:62,500.

Woodford, A.O., and Gander, Craig, 1977, Los Angeles erosion surface of Middle Cretaceous age: American Association of Petroleum Geologists Bulletin, v. 61, p. 1979-1990.

Wright, T.L., 1991, Structural Geology and Tectonic Evolution of the Los Angeles Basin, California, *in* Active Margin Basins, K.T. Biddle, *ed*., American Association of Petroleum Geologists Memoir 52, 35-134.

Yerkes, R.F., McCulloh, T.H., Schoelhamer, J.E., and Vedder, J.G.,1965, Geology of the Los Angeles basin—an introduction: U.S. Geological Survey Professional Paper 420-A, 57 p.

Yerkes, R.F., 1972, Geology and oil resources of the western Puente Hills area, southern California: U.S. Geological Survey Professional Paper 420-C, 63 p.

Zawila, J.S., 1996, Gravity mapping of subsurface structures in the central Perris tectonic block, southern California: Riverside, University of California, Master's thesis.

Ziony, J.K., and Yerkes, R.F., 1985, Evaluating earthquake and surface faulting potential in J.I. Ziony, *ed*., Evaluating earthquake hazards in the Los Angeles region—an earth-science perspective: U.S. Geological Survey Professional Paper 1360, p. 43-91.

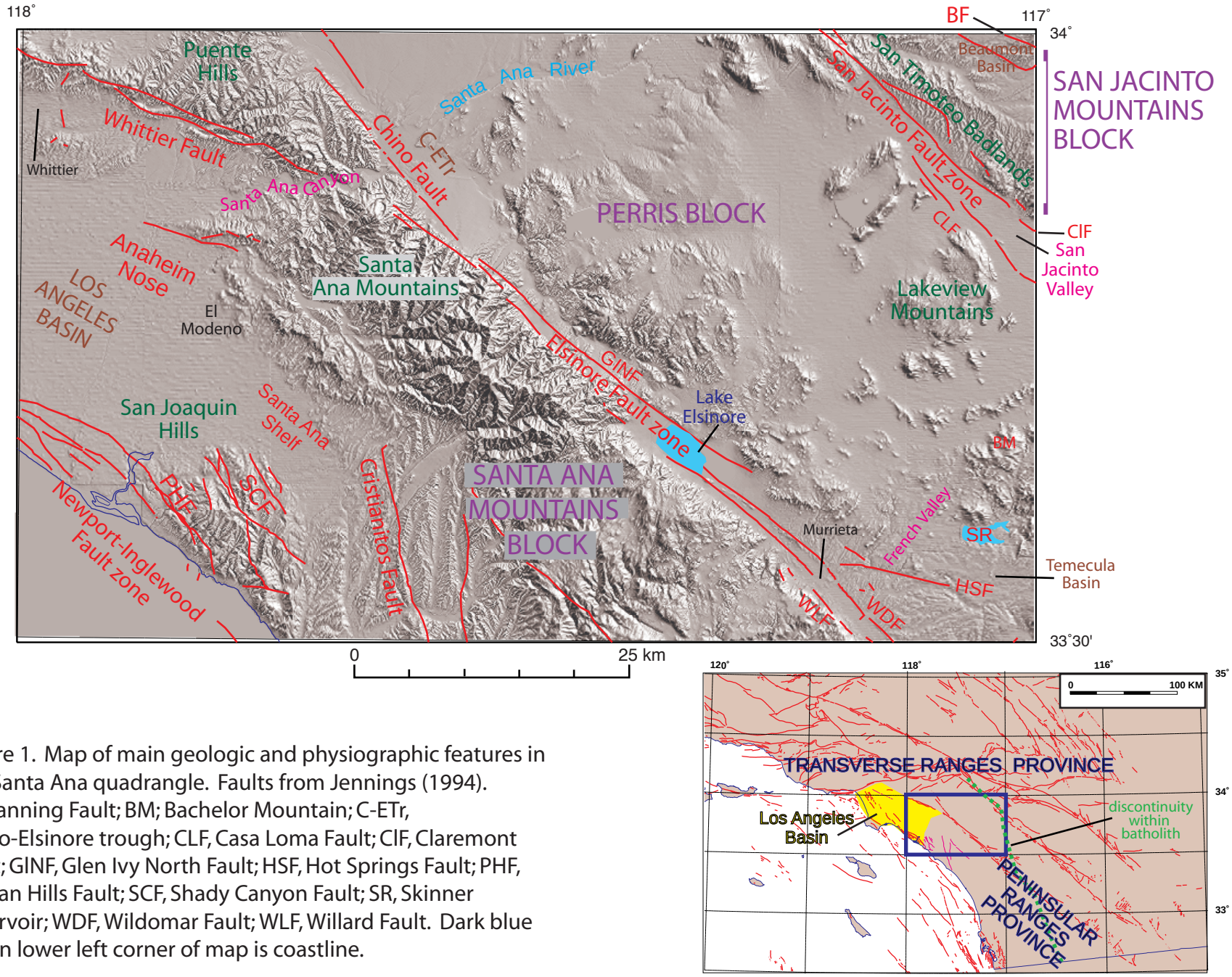

Figure 1. Map of main geologic and physiographic features in the Santa Ana quadrangle. Faults from Jennings (1994). BF, Banning Fault; BM; Bachelor Mountain; C-ETr, Chino-Elsinore trough; CLF, Casa Loma Fault; ClF, Claremont Fault; GlNF, Glen Ivy North Fault; HSF, Hot Springs Fault; PHF, Pelican Hills Fault; SCF, Shady Canyon Fault; SR, Skinner Reservoir; WDF, Wildomar Fault; WLF, Willard Fault. Dark blue line in lower left corner of map is coastline.

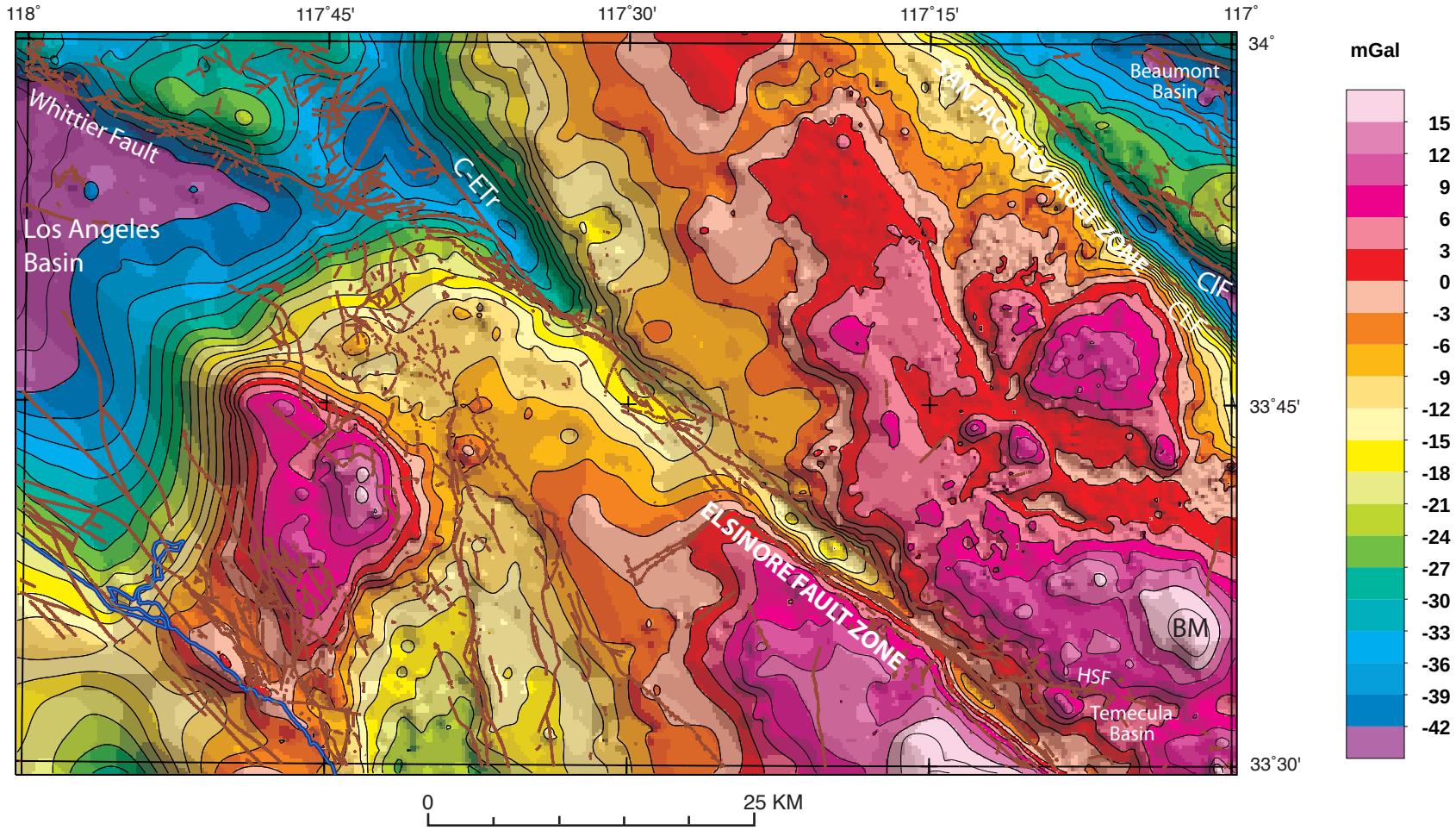

Figure 2. Color-contour isostatic gravity map. Brown lines are faults. Blue line denotes coastline. Illumination from the northeast, which highlights northwest-striking features. See figure 1 for explanation of abbreviations.

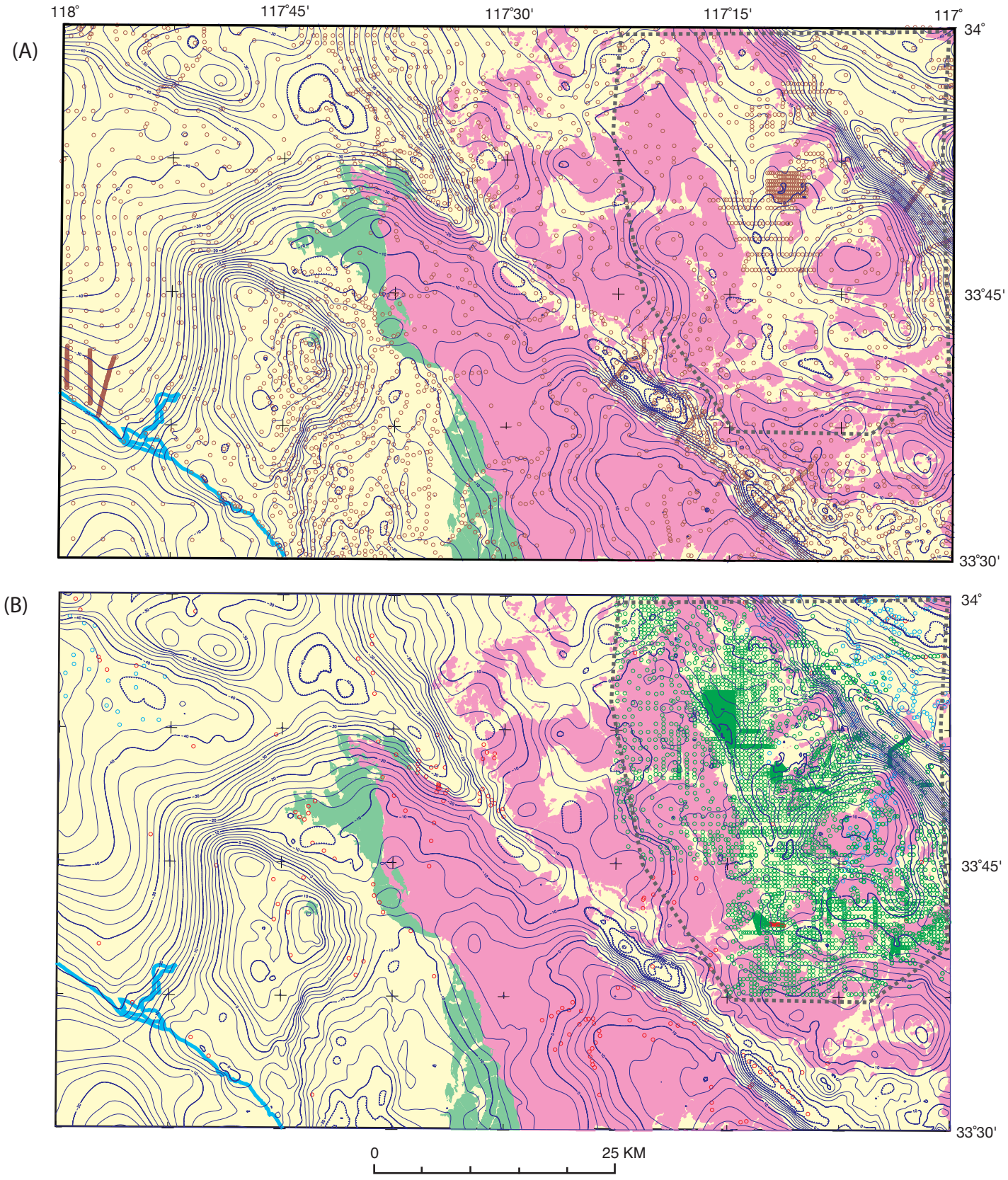

Figure 3. Comparison of (A) gravity field from Langenheim and others (1991) and (B) gravity field from this report. Contour interval, 2 mGal. Brown circles on (A) are data from Langenheim and others (1991); red, green, and blue circles are new data from National Geodetic Survey, University of California, Riverside, and U.S. Geological Survey, respectively. Pink and green areas are exposures of pre-Cenozoic crystalline and sedimentary rocks, respectively. The most significant improvement in resolution of the gravity field is located in eastern third of the quadrangle. Compare area marked by dark gray dashed line on (A) and (B). Coastline showin in blue.

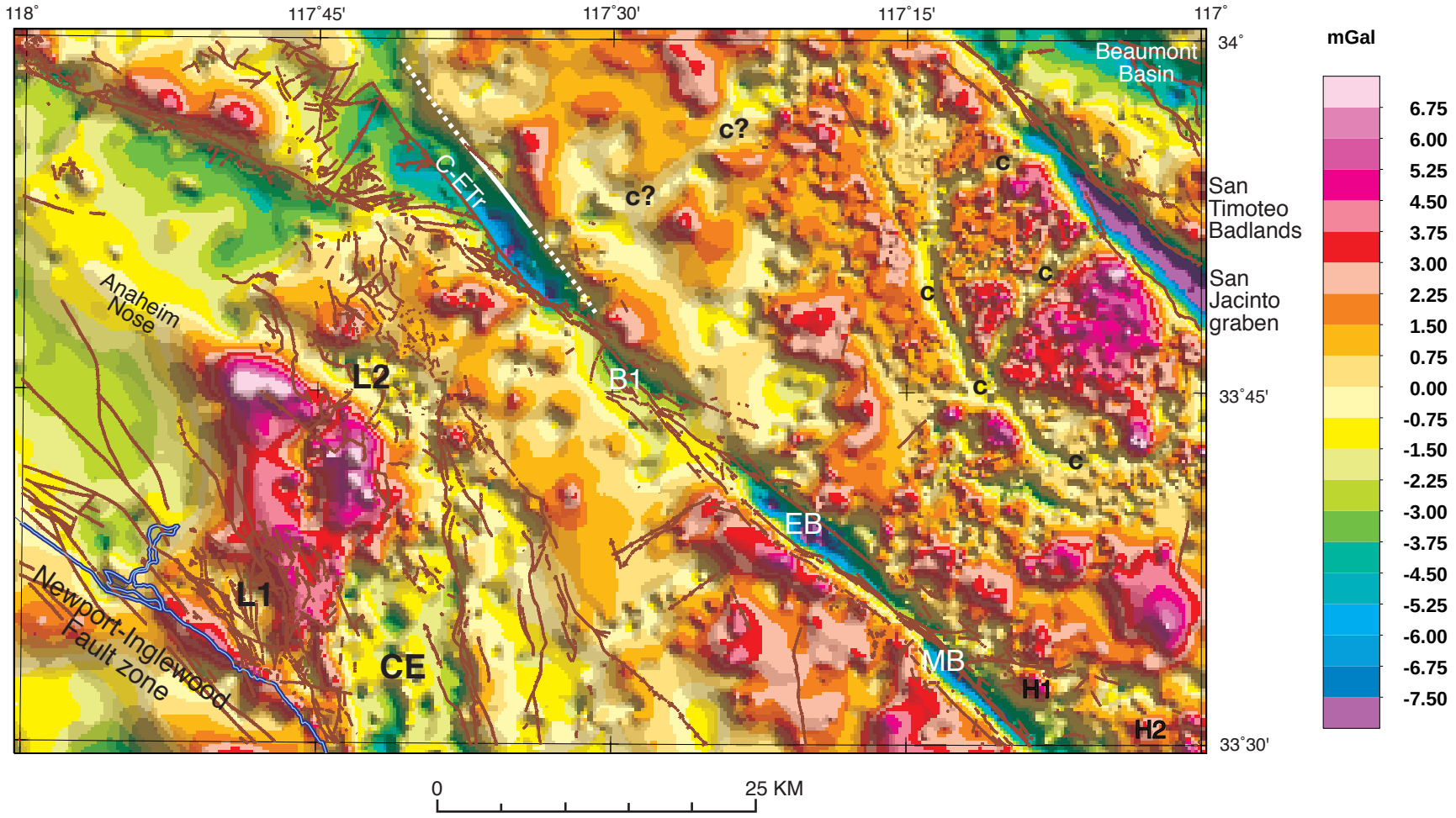

Figure 4. Residual gravity map. Brown lines are faults. Blue line is the coastline. White dashed line is gravity gradient of the "Chino Hingeline" Fault, dashed where projected beyond previously inferred trace. CE, Capistrano embayment gravity low; L1, gravity low between Shady Canyon and Pelican Hills Faults; L2, gravity low between Santa Ana Mountains and northern margin of the San Joaquin gravity high. EB, basin beneath Lake Elsinore, MB, Murrieta basin, B1, small basin northwest of EB discussed in text. H1 and H2 are local gravity highs within the Temecula Basin. "c" are inferred paleochannels.

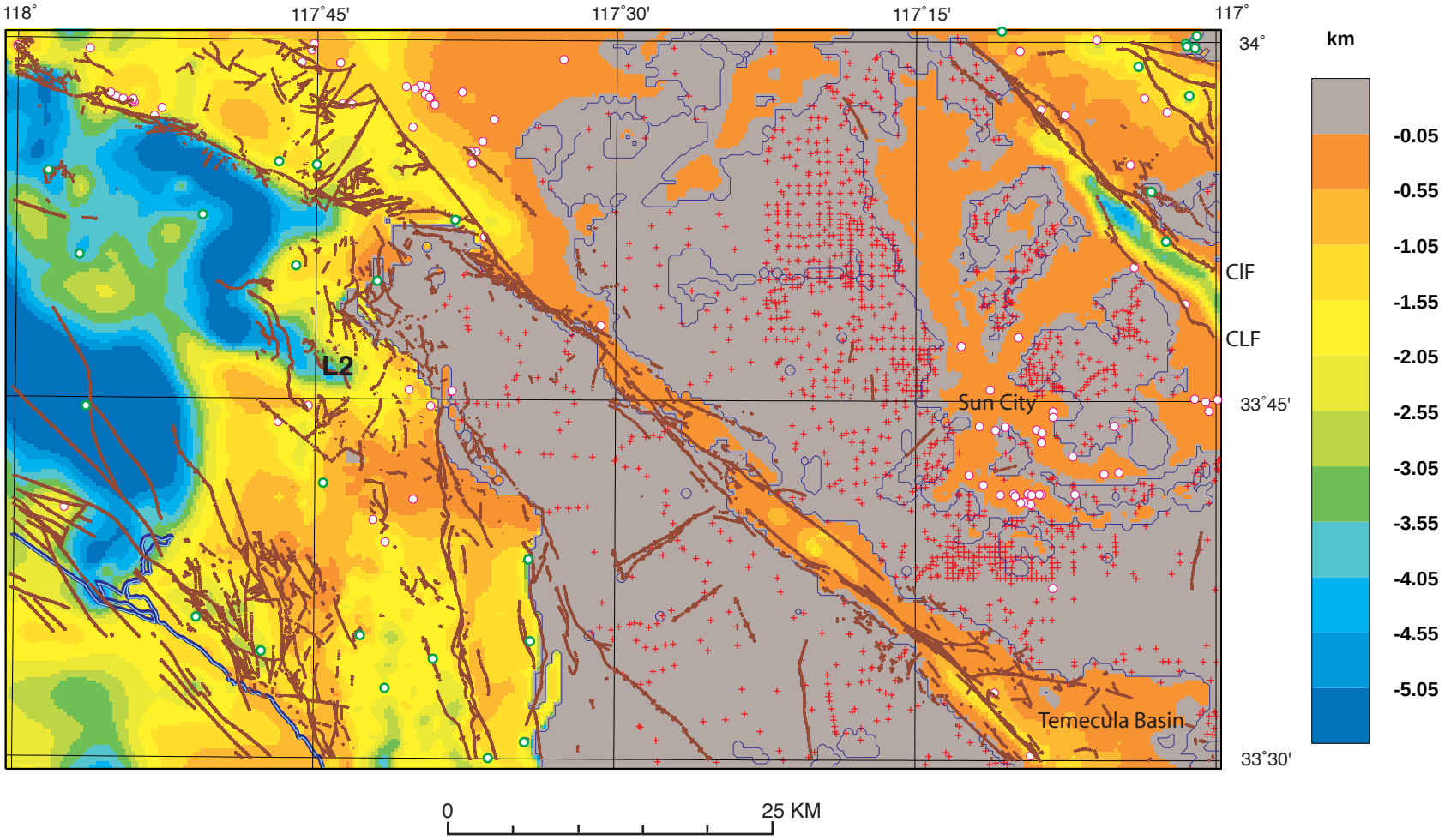

Figure 5. Basin thickness map. Brown lines are faults. Thin blue line is pre-Cenozoic igneous and metamorphic basement contact. Magenta-rimmed white circles are wells that penetrated basement and thus could be used to constrain the inversion. Red crosses are gravity stations measured on basement. Green-rimmed circles are wells that did not penetrate basement. See figure 1 for explanation of abbreviations.

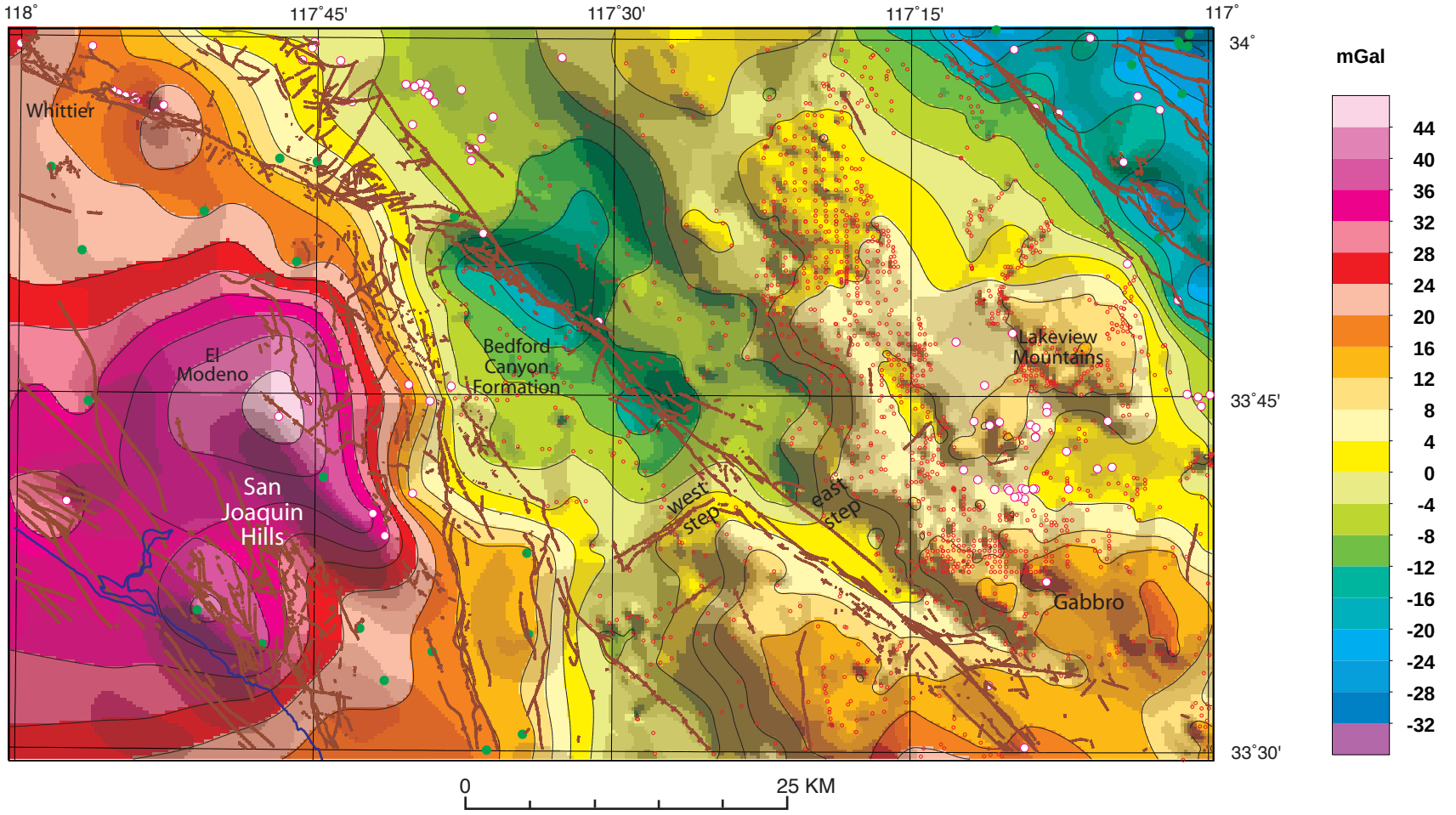

Figure 6. Basement gravity map. Brown lines are faults. Magenta-rimmed white circles are wells that penetrate basement rock. Red circles are gravity stations measured on basement. Green circles are wells that do not penetrate basement. Increasing basement gravity values southeastward across the Santa Ana Mountains and Perris blocks are marked by "west step" and "east step," respectively.